Ultrasonics Sonochemistry 82 (2022) 105886

Contents lists available at ScienceDirect

Ultrasonics Sonochemistry

journal homepage: www.elsevier.com/locate/ultson

Effect of ultrasound on the kinetics of anti-solvent crystallization of sucrose

Xuwei Zhong [a,b], Chengdu Huang [a,b,*], Lishan Chen [a,b], Qinghong Yang [a,b], Yongchun Huang [a,b,*]

[a] Guangxi Key Laboratory of Green Processing of Sugar Resources (Guangxi University of Science and Technology), Liuzhou 545006, China
[b] Province and Ministry Co-sponsored Collaborative Innovation Center of Sugarcane and Sugar Industry, Nanning 530004, China

ARTICLE INFO

Keywords:
Ultrasound
Sucrose
ASL model
Crystallization kinetics

ABSTRACT

The effect of ultrasound on the kinetics of anti-solvent crystallization of sucrose was studied. The influence of temperature, stirring rate, supersaturation and ultrasonic power on the anti-solvent crystallization of sucrose was investigated. The relationship between infrared spectral characteristic band of sucrose and supersaturation was determined with an online reaction analyzer. The crystal size distribution of sucrose was detected by a laser particle-size analyzer. Ultrasound accelerated the crystallization process, and had no impact on the crystal shape. Abegg, Stevens and Larson model was fitted to the experimental data, and the results were the following: At 298.15 K, the average size of crystals was 133.8 μm and nucleation rate was 4.87×10^{9} $m^{-3} \cdot s^{-1}$ without ultrasound. In an ultrasonic field, the average size was 80.5 μm, and nucleation rate was 1.18×10^{11} $m^{-3} \cdot s^{-1}$. Ultrasound significantly reduced the average size of crystals and improved the nucleation rate. It was observed that the crystal size decreased with the increase of stirring rate in silent environment. When the stirring rate increased from 250 to 400 rpm, the average size decreased from 173.0 to 132.9 μm. However, the stirring rate had no significant impact on the crystal size in the ultrasonic field. In addition, the activation energy of anti-solvent crystallization of sucrose was decreased, and the kinetic constant of nucleation rate was increased due to the effect of ultrasound. In the ultrasonic field, the activation energy was reduced from 20422.5 to 790.5 $J \cdot mol^{-1}$, and the kinetic constant was increased from 9.76×10^{2} to 8.38×10^{8}.

1. Introduction

Sucrose crystallization is vital for sugar production. The methods and applications of sucrose crystallization are the key of scholars' research [1–4]. The crystallization can be affected by seed, temperature, additives or impurities, stirring rate and ultrasound [5–9]. The general methods of sucrose crystallization are seeding and natural crystallization. However, there are also many disadvantages such as long crystallization time and large energy loss. Anti-solvent crystallization can overcome these limitations and provide better choices. Meanwhile, other auxiliary means such as ultrasound were used in industry to intensify the crystallization process, because it can further reduce solvent consumption and control crystal size.

The application of ultrasound in the crystallization process has received extensive attention in recent years, and was regarded as an important factor affecting nucleation. Ultrasound can accelerated the crystallization process, and change the crystal shape [10]. In supersaturated crystallization, ultrasound can improve the nucleation rate and control the growth of crystals [11]. Amara et al. [12] studied the growth of potash alum crystals in silent environment as well as in the ultrasonic field. It was proved that the value of kinetic parameter g of crystal growth in the ultrasonic field was smaller than that in silent environment, but it was always superior to 1. Vera et al. [13] investigated the effect of ultrasound on the anti-solvent crystallization of α-glycine. The de-supersaturation rate was increased due to the influence of ultrasound, resulting in a higher nucleation rate, a higher growth rate or both. The crystallization time was only 40 min in the ultrasonic field. However, the crystallization time needed 120 min in silent environment. Khaire and Gogate [14,15] understood the effect of different ultrasonic reactors on the recovery of lactose using crystallization, and proposed a new method to improve the recovery of lactose in whey based on different pretreatment technologies. The references showed that the ultrasonic bath had higher crystallization recovery than the ultrasonic horn in the laboratory scale. In the large system, the dual-frequency ultrasonic reactor was proved to have higher lactose recovery. Compared with thermal and ultrasonic pretreatments, thermosonication pretreatment had the maximum lactose recovery. Gajendragadkar and Gogate [16] found that the purity and recovery of lactose were increased in a relatively short time due to the presence of ultrasound. In the

* Corresponding authors at: Guangxi Key Laboratory of Green Processing of Sugar Resources (Guangxi University of Science and Technology), Liuzhou 545006, China.
E-mail addresses: gx-hcd@163.com (C. Huang), huangyc@yeah.net (Y. Huang).

https://doi.org/10.1016/j.ultsonch.2021.105886
Received 14 November 2021; Received in revised form 18 December 2021; Accepted 21 December 2021
Available online 27 December 2021

Nomenclature

b	ASL model parameters (−)
B°	nucleation rate ($m^{-3}\cdot s^{-1}$)
k_B	kinetic constant of nucleation rate (−)
i	order of supersaturation level (−)
j	order of suspension density (−)
l	order of stirring rate (−)
G	overall linear growth rate ($m\cdot s^{-1}$)
G°	growth rate of nuclei (ASL model) ($m\cdot s^{-1}$)
g	order of growth rate (−)
k_G	overall growth rate constant (−)
ΔS	supersaturation level (−)
M_T	suspension density of solution ($kg\cdot m^{-3}$)
N_p	stirring rate (rpm)
E_a	activation energy ($J\cdot mol^{-1}$)
R	gas mole constant ($J\cdot mol^{-1}\cdot K^{-1}$)
L	crystal size (m)
T	temperature (K)
n	population density (m^{-4})
K_v	volume shape factor (−)
V	volume (m^3)
t	time (s)
ΔL_i	width of the i-th particle size interval (m)
$\overline{L_i}$	average particle size of the i-th particle size interval (m)
Y	actual solubility of sucrose in pure water at a certain temperature ($g_{sucrose}\cdot g_{water}^{-1}$)
Y_0	saturation solubility of sucrose at the same temperature ($g_{sucrose}\cdot g_{water}^{-1}$)

Greek letters

γ	ASL model parameters (−)
ρ	crystal density ($kg\cdot m^{-3}$)
τ	residence time (s)

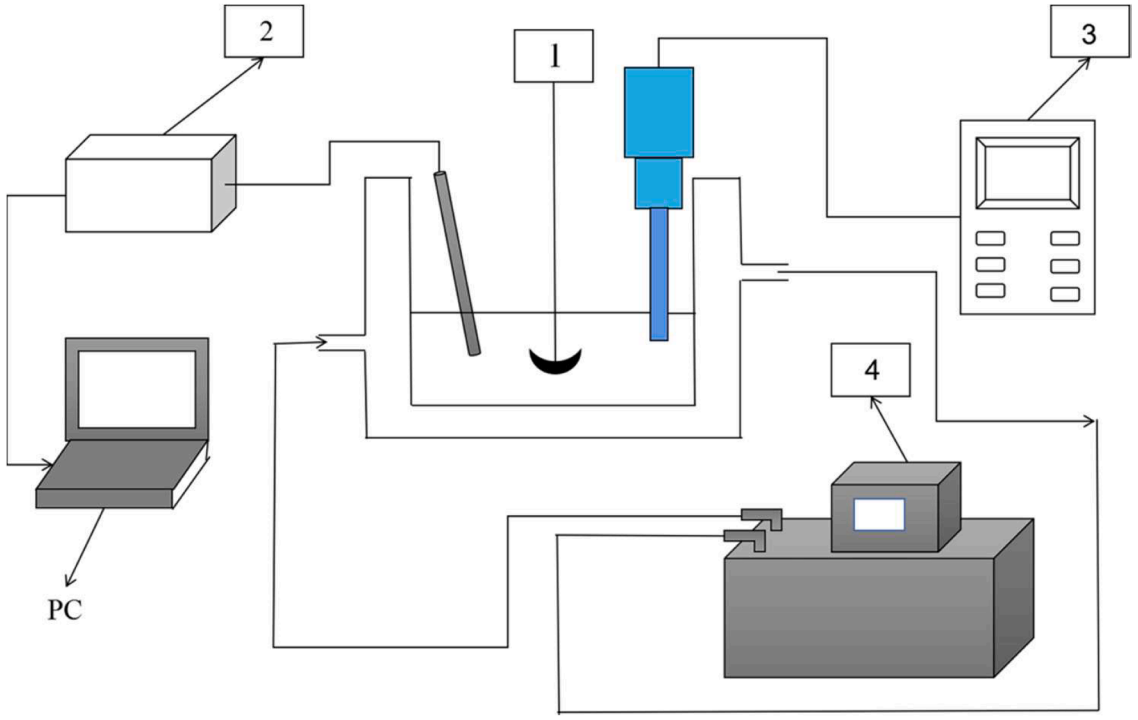

Fig. 1. Schematic graph of experimental devices: (1) electric stirrer, (2) online reaction analyzer, (3) multi-frequency ultrasonic apparatus, (4) thermostatic equipment.

Table 1
Solubility of sucrose in pure water at different temperatures.

T (K)	Solubility ($g_{sucrose}\cdot g_{water}^{-1}$)
298.15	2.094
302.15	2.158
306.15	2.229
310.15	2.307

ultrasonic bath, the purity of lactose was increased with the increase of frequency, but the recovery was decreased. Nalajala et al. [17] showed that the convective properties in the medium were the key factors affecting the nucleation and growth rates, and further affected the crystal size distribution (CSD). Compared with the CSD of mechanical stirring system, the main crystal size of ultrasonic crystallization system was smaller, but the span of CSD was larger. Devos et al. [18] studied the nucleation kinetics of primary, secondary and ultrasound-induced paracetamol in stirred microvials, and proved that the nucleation kinetics was affected due to the introduction of ultrasound in the crystallization process. In the absence of stirring rate, ultrasound-induced nucleation can effectively replace seeding. Ramisetty et al. [19] established the kinetics of anti-solvent crystallization of benzoic acid by measuring the change of crystal size with time. It was observed that the parameters of the nucleation and growth rates were of great significance in the modeling of anti-solvent crystallization. Sayan et al. [20] calculated the kinetics of crystallization of potassium dihydrogen phosphate in continuous crystallization system by Abegg, Stevens and Larson (ASL) model, and found that ultrasound significantly improved the nucleation

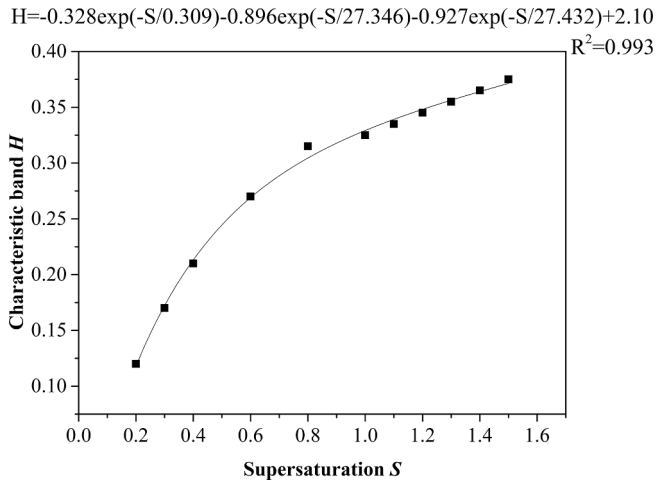

Fig. 2. Relationship between infrared spectral characteristic band (H) and supersaturation (S) (T = 298.15 K).

rate of the system. Hatkar et al. [21] investigated the effect of ultrasound on anti-solvent crystallization of salicylic acid, and proved that the exact time of application of ultrasound altered the average particle size of crystals and significantly affected the agglomeration of crystals. In the overview of studies, the positive role of ultrasound in solution crystallization was described, but the research direction was mainly focused on the crystal size, induction time and so on. The effect of ultrasound on crystallization kinetics and activation energy of sucrose was lacking clearly establishing the novelty of the current work.

The author found that the nucleation rate was higher and the crystallization time was shorter in the ultrasonic field than that in silent environment. Under the same conditions, the crystals in the ultrasonic field may be broken, resulting in the measurement error of CSD. So it was difficult to compare the CSD in the same time. In order to overcome these difficulties, the relationship between infrared spectral characteristic band of sucrose and supersaturation was determined with an online reaction analyzer. Under the same condition of supersaturation level, the kinetics of anti-solvent crystallization of sucrose was studied in silent and ultrasonic environments. The ASL model was used to clarify the effect of ultrasound on population density, nucleation and growth rates.

2. Materials and methods

2.1. Materials

The sucrose was provided by Fengtang Biochemical Co., Ltd (Guangxi, China), and its quality was grade one. Anhydrous ethanol (Analytical Pure) was purchased from Kelong Chemical Co., Ltd (Chengdu, China). Glycerol (Analytical Pure) was purchased from Xilong Science Co., Ltd (China). Sucrose ester (SE-15) was purchased from Wanbang Industrial Co., Ltd (Guangxi, China).

2.2. Methods

2.2.1. Experimental devices and methods of anti-solvent crystallization of sucrose

The experimental setup was shown in Fig. 1. The experiments were performed in a jacketed vessel of 500 mL. The supersaturated solution of sucrose at different temperatures was prepared by Table 1. At 363.15–373.15 K, sucrose was completely dissolved in pure water (75 g). Then, the sucrose solution was cooled to experimental temperature to obtain a supersaturated solution. Sucrose solution (197.6 g) was poured into the jacketed vessel and then the anti-solvent (79 g ethanol, 15.8 g glycerol and 0.04 g sucrose ester) was added. Experiments were conducted at four different temperatures (T), four different stirring rates (N_p), five different supersaturations (S) and four different ultrasonic powers (W). Electric stirrer (Zhengzhou Yuxiang Equipment, S312-120

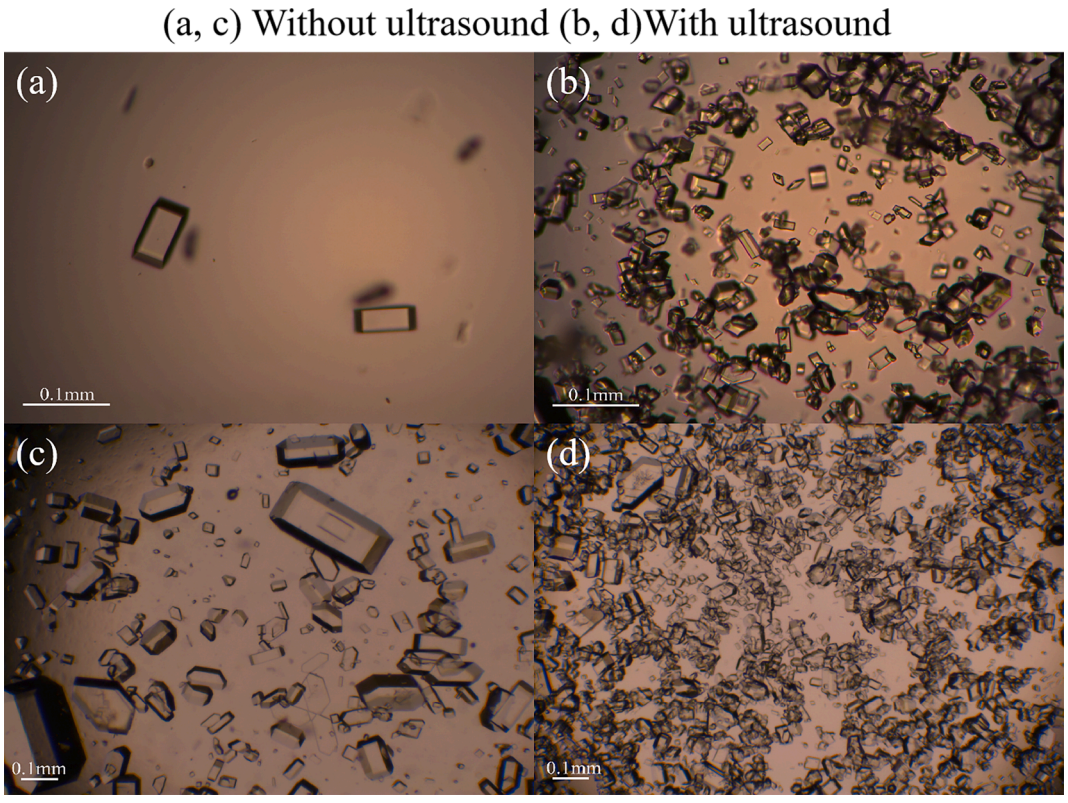

Fig. 3. Shape and population density of sucrose crystals (T = 306.15 K, N_p = 350 rpm, S = 1.3, P = 108 W, t_0 = 16 min).

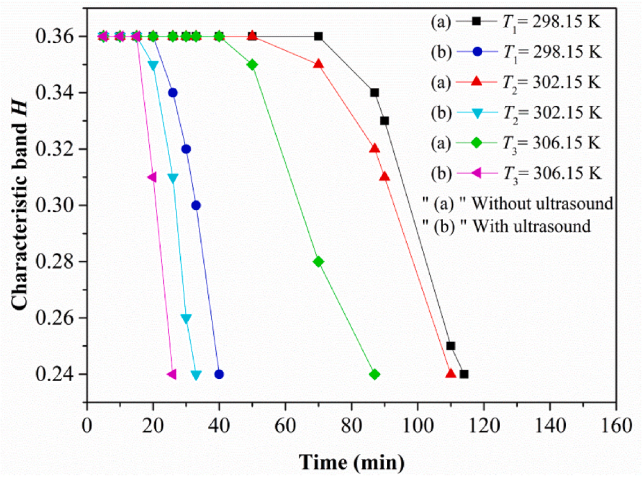

Fig. 4. Effect of temperature on the crystallization time (N_p = 300 rpm, S = 1.3, ΔS= 0.816, P = 108 W, t_0 = 16 min).

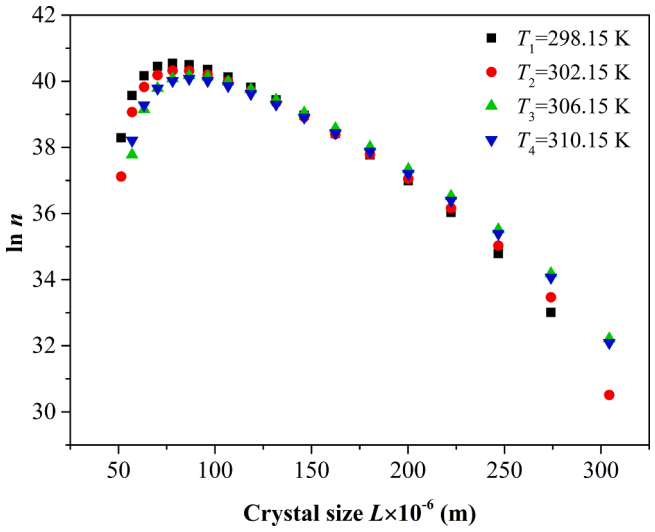

Fig. 5. Population density graph of sucrose crystallization (N_p = 300 rpm, S = 1.3, ΔS= 0.816).

Table 2
ASL model parameters for sucrose crystallization without ultrasound at different temperatures.

T (K)	ln n°	γ	b
298.15	39.7	0.00547	−3.03
302.15	39.2	0.00446	−3.71
306.15	39.2	0.00475	−3.23
310.15	39.4	0.00538	−2.80

Notes: S = 1.3, N_p = 300 rpm, ΔS= 0.816

W) was used to produce different stirring rates. Temperature control in the vessel was achieved by a thermostatic equipment (Changzhou Henglong Instrument, HH-601). Online reaction analyzer (Mettler-Toledo, React IR702L) was used to control the supersaturation level. Multi-frequency ultrasonic apparatus (Nanjing Shunliu Instrument, SL-650SD) was used to produce different ultrasonic powers. Anti-solvent and sucrose solution should be mixed before turning on the ultrasound and timing. The frequency of the equipment was 30 kHz, and the ultrasonic mode was set to turn on for 1 s and turn off for 1 s. The ultrasonic time (t_0) was set to 16 min. The ultrasonic energy was introduced

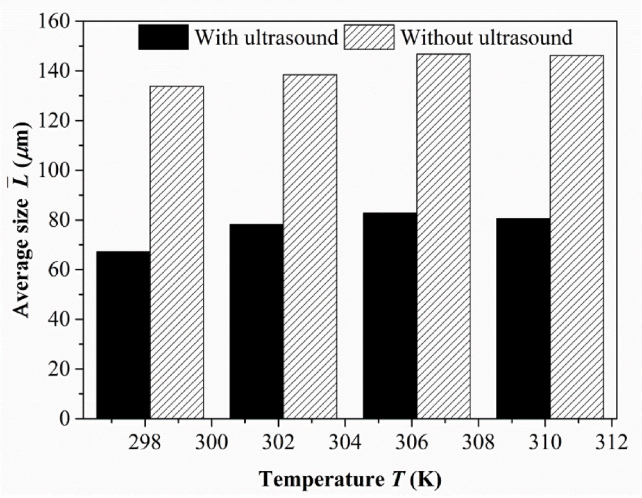

Fig. 6. Effect of temperature on average size (N_p = 300 rpm, S = 1.3, ΔS= 0.816, P = 108 W, t_0 = 16 min).

into the crystallization system by a conical ultrasonic generator with a diameter of 10 mm.

2.2.2. Measurement of supersaturation level

At 298.15 K, different supersaturated solutions (197.6 g) and anti-solvent were added to the beaker. When sucrose solution was completely mixed with anti-solvent, the relationship between infrared spectral characteristic band (H) at 990 cm^{-1} and supersaturation (S) was determined with an online reaction analyzer. The relationship was shown in Fig. 2. The fitting curve was determined with the specific mathematical model. The reason was that the results of general linear fitting deviated greatly from the experimental results, while the fitting curve using specific mathematical model was the closest to the experimental results. The kinetic model established by Sayan [20] was generally replaced by the growth rate due to the difficulty of measuring the supersaturation level. In the present work, the model was simplified and the supersaturation level was calculated accurately due to the establishment of the fitting curve.

2.2.3. Observation of sucrose crystals

During the crystallization process, two drops of the solution were withdrawn and dispersed on a glass slide every five minutes. The shape and quantity of crystals were observed and taken by Leica system (DM 2000).

2.2.4. Measurement of CSD

The timing was stopped when the H value was reduced to 0.24 or stopped decreasing. The solution of 5 mL was filtered and then dried. The sucrose sample was dispersed in absolute ethanol. The mixture was added to a cuvette. The crystal size distribution (CSD) of sucrose was determined with a laser particle-size analyzer (Liaoning Instrument, GSL-1010).

3. Model formulation

The nucleation rate (B) is the number of new particles formed per unit time per unit volume of solution [20]. It is affected from supersaturation level (ΔS), suspension density (M_T) and stirring rate (N_p). Under condition of supersaturation, these effects can be given below:

$$B = k_B exp\left(-\frac{E_a}{RT}\right)\Delta S^i M_T^j N_p^l \quad (1)$$

where S = $\frac{Y}{Y_0}$, Y is the actual solubility of sucrose in pure water at a

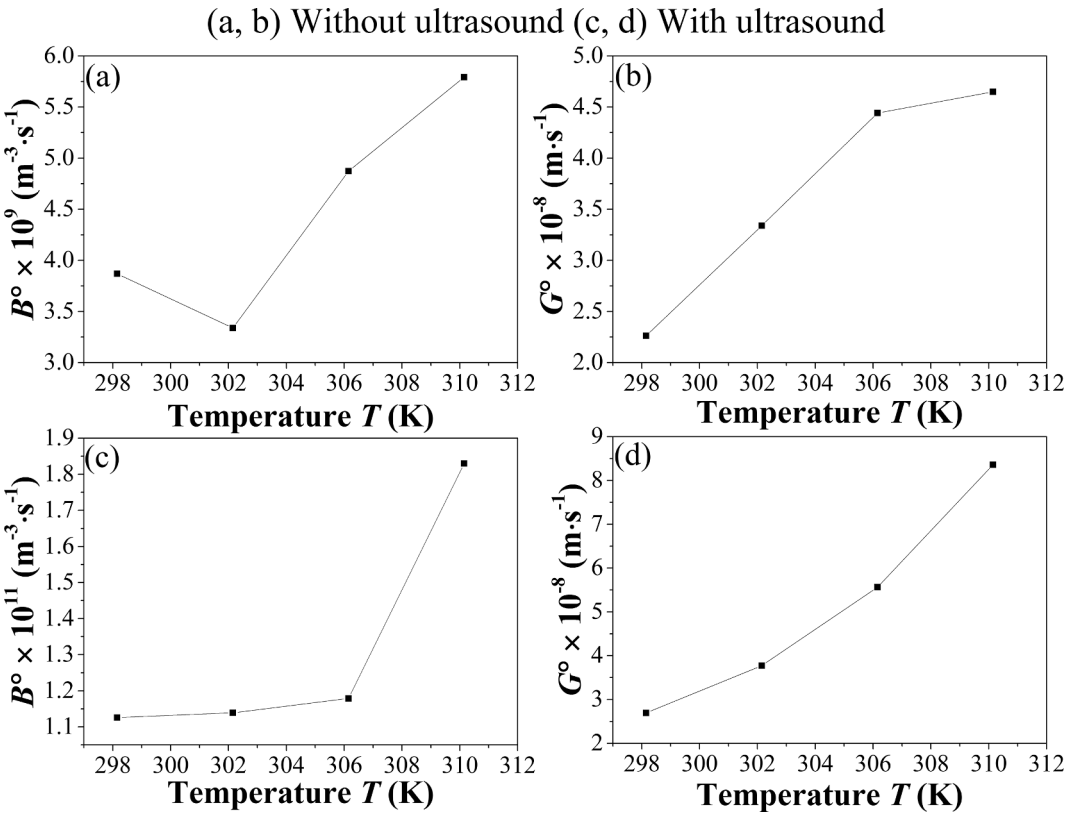

Fig. 7. Effect of temperature on the nucleation and growth rates (S = 1.3, N_p = 300 rpm, ΔS= 0.816, P = 108 W, t_0 = 16 min).

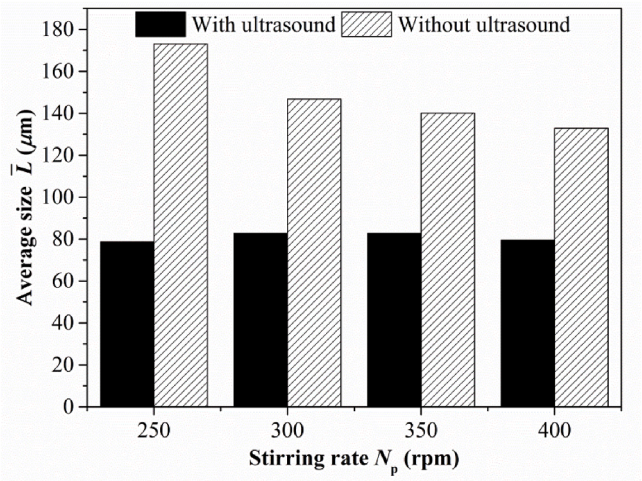

Fig. 8. Effect of stirring rate on average size (T = 306.15 K, S = 1.3, ΔS= 0.816, P = 108 W, t_0 = 16 min).

certain temperature, Y_0 is the saturation solubility of sucrose at the same temperature. After formation of stable nuclei, they begin to grow into visible crystals. Two steps in mass deposition process are suggested. These are the diffusion from bulk of the solution to crystal surface and the reaction on the crystal surface. The overall growth rate (G) is the rate of change of the crystal size (L) with time and is expressed as [22]:

$$G = \frac{dL}{dt} = k_G \Delta S^g \tag{2}$$

The number of crystals corresponding to the particle size L is called the population density (n). The population density can be expressed as:

$$\frac{dnG}{dL} + \frac{n}{\tau} = 0 \tag{3}$$

where τ is the residence time. Eq. (3) is the steady-state particle size balance calculation formula of mixed-suspension mixed-product removal crystallizer (MSMPR). Here, both agglomeration and attrition are neglected. If the growth rate is size independent, Mc Cabe's ΔL law [20] is expressed as follows:

$$n = n^{\circ} exp\left(-\frac{L}{G\tau}\right) \tag{4}$$

where n° is the population density of the crystals when size is zero. The crystal growth rate may be determined from the slope of logarithmic plot of population density while the intercept of the line gives the value of ln n°. The nucleation rate can be determined as:

$$B = n^{\circ} G \tag{5}$$

and the kinetic orders i, j and l can be determined from Eq. (1). If the growth rate is size dependent, researchers have proposed many models such as the Bramson and Canning-Randolph models, etc. However, the ASL model has a wide range of adaptability, and Abegg, Stevens and Larson suggested that the size-dependent growth rate could be described as follows:

$$G(L) = G^{\circ}(1 + \gamma L)^b \tag{6}$$

where G° is the growth rate of the crystal nucleus, γ and b are parameters. Combining Eq. (6) with Eq. (3), the equation of population density can be obtained:

$$n = n^{\circ}(1 + \gamma L)^{-b} exp\left[\frac{1 - (1 + \gamma L)^{1-b}}{1 - b}\right] \tag{7}$$

Eq. (7) can be rewritten as:

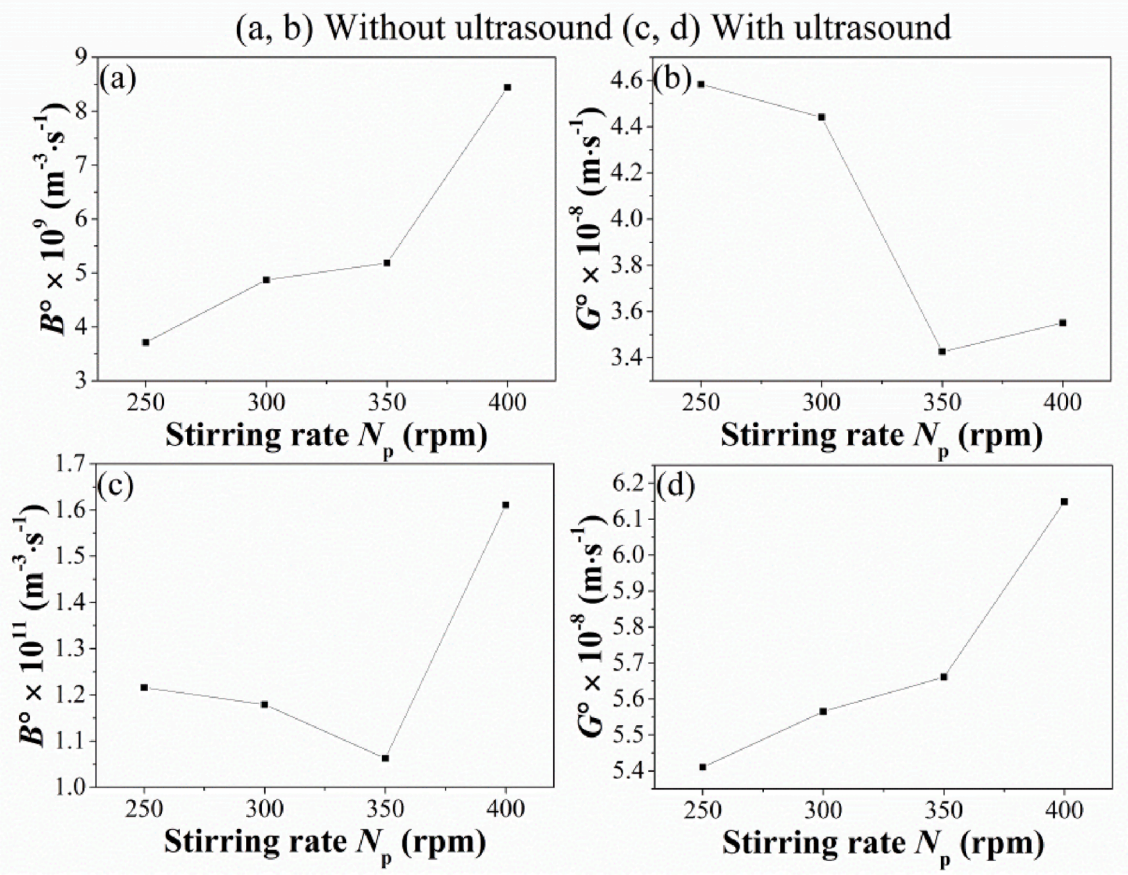

Fig. 9. Effect of stirring rate on the nucleation and growth rates (T = 306.15 K, S = 1.3, ΔS= 0.816, P = 108 W, t_0 = 16 min).

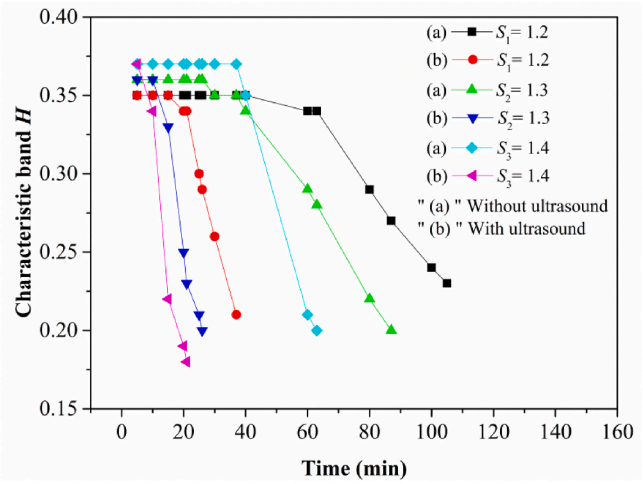

Fig. 10. Effect of supersaturation on crystallization time (T = 306.15 K, N_p = 300 rpm, H no longer decreased, P = 108 W, t_0 = 16 min).

$$lnn = lnn^\circ + \frac{1}{1-b} - bln(1+\gamma L) - \frac{(1+\gamma L)^{1-b}}{1-b} \tag{8}$$

where $\gamma = \frac{1}{G^\circ \tau}$. In this case, the nucleation rate can be determined using the following equation:

$$B^\circ = n^\circ \cdot G^\circ \tag{9}$$

Based on the CSD of sucrose obtained in 2.2.4, the population densities of sucrose crystals in different particle sizes are given by the following equation:

$$n_i = \frac{wM_T}{\rho K_V \overline{L_i}^3 \Delta L_i} \tag{10}$$

where w is the volume fraction of the i-th particle size interval, M_T is the suspension density of solution, K_v is the volume shape factor, ρ is the crystal density, ΔL_i is the width of the i-th particle size interval, and $\overline{L_i}$ is the average particle size of the i-th particle size interval.

Volume shape factor can be given as:

$$K_V = \frac{V_3 - V_2}{V_1} \tag{11}$$

where V_1 is the volume of sucrose crystals of a given mass, V_2 is the volume of anhydrous ethanol, and V_3 is the mixing volume of sucrose crystals and absolute ethanol.

4. Results and discussion

4.1. Effect of ultrasound on the population density and crystal size

Fig. 3a and b illustrated the shape and population density of sucrose crystals when the crystallization time was 20 min. Fewer hexagonal sucrose crystals were observed in silent environment compared with the ultrasonic environment. Ultrasound had no impact on the crystal shape, which was similar to the results obtained by Singh [23]. Fig. 3c and d showed the shape and population density of sucrose crystals under the same condition of supersaturation level. The crystal size was smaller in the ultrasonic field than that in silent environment. So ultrasound shortened the crystallization time and reduced the crystal size. Kim et al. [24] also believed that ultrasound shortened the induction time by

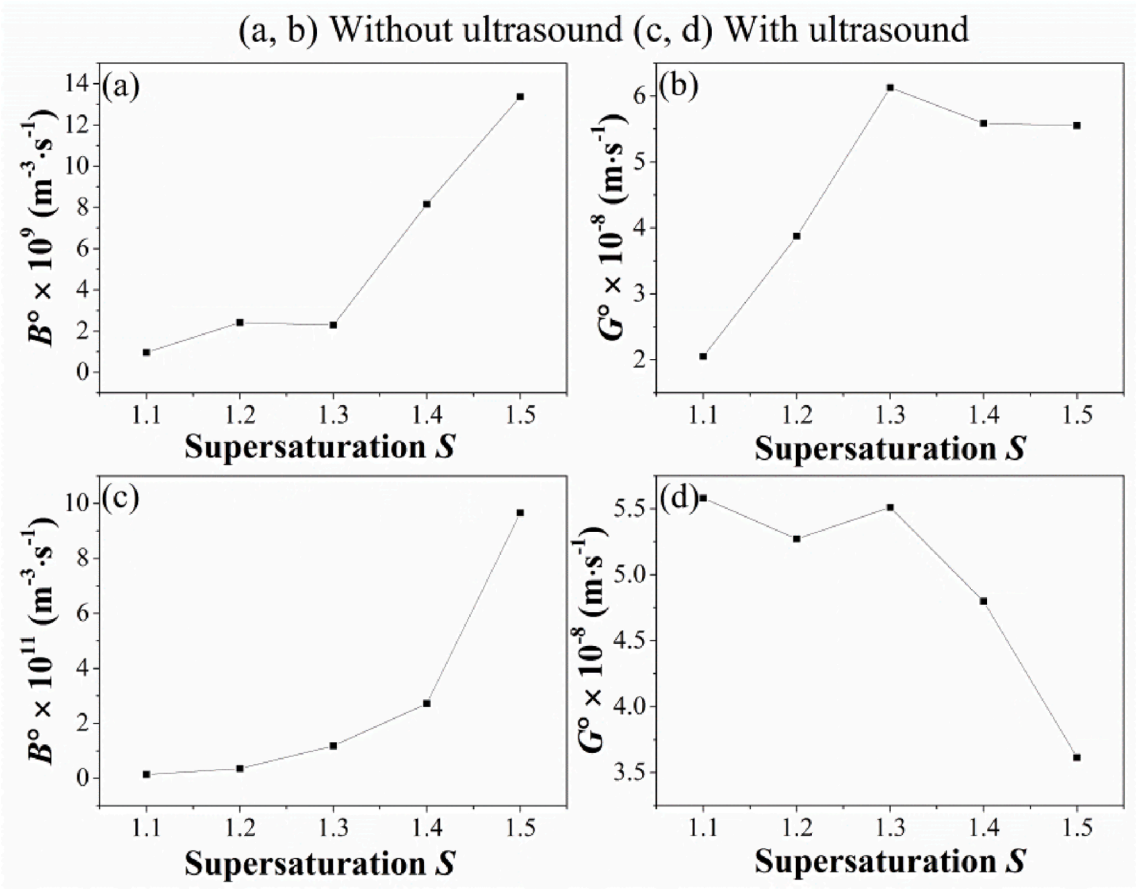

Fig. 11. Effect of supersaturation on the nucleation and growth rates (T = 306.15 K, N_p = 300 rpm, H no longer decreased, P = 108 W, t_0 = 16 min).

improving the micro-scale mixing and turbulence caused by acoustic cavitation. With the decrease of induction time, the crystals appeared faster. Therefore, the number of crystals generated was increased and the crystal size was decreased.

4.2. Effect of temperature

The effect of temperature on the crystallization time was shown in Fig. 4. It can be seen that Fig. 4a and b represented crystallization time in silent and ultrasonic environments. The crystallization time was shortened with the increase of temperature. The reason may be that the molecules had high mobility and energy at high temperatures [25], resulting in faster nucleation rate and lower crystallization time. The population density at different temperatures was shown in Fig. 5. The results of population density indicated a deviation from linearity, and roughly showed a downward trend. Similar behaviors in population density were observed for all of the applied ultrasonic power degrees. So the ΔL law cannot be used for data analysis. In this paper, the ASL model was used to calculate the population density, and Eq. (8) was fitted to the data of population density to obtain the model parameters γ, n° and b. It can be seen from Table 2 that all the b values were minus, meaning the growth rate increased with the increase of volume [20].

The effect of temperature on the average size was shown in Fig. 6. The average size was 133.8 μm at 298.15 K, 138.4 μm at 302.15 K, 146.8 μm at 306.15 K and 146.2 μm at 310.15 K in silent environment, while the average size was 67.2 μm at 298.15 K, 78.3 μm at 302.15 K, 82.7 μm at 306.15 K and 80.5 μm at 310.15 K in the ultrasonic field. The results showed that the average size was increased with the increase of temperature. Increasing temperature was conducive to the growth of crystals, and improved the growth rate. At 310.15 K, the average size no longer increased and tended to be stable.

The effect of temperature on the nucleation and growth rates was shown in Fig. 7. It was observed that Fig. 7a and b showed the nucleation and growth rates in silent environment, while those in the ultrasonic environment were shown in Fig. 7c and d. It was clearly seen that the nucleation and growth rates were increased due to the increase of temperature. For the same initial supersaturation in the solutions, higher temperatures also resulted in a lower solution viscosity which led to a higher molecular diffusion rate, consequently, accelerating the reaction rate [26]. At 298.15–306.15 K, the ultrasonic field had a minor effect on the nucleation rate. The effect was provoked at above 310.15 K.

4.3. Effect of stirring rate

The effect of stirring rate on the average size was shown in Fig. 8. The average size was 173.0 μm at 250 rpm, 146.8 μm at 300 rpm, 140.1 μm at 350 rpm and 132.9 μm at 400 rpm in silent environment. It can be seen that the stirring rate had a significant impact on the average size. The average size was reduced with the increase of stirring rate. The reason may be that lower stirring rate can reduce the nucleation and promote the formation of large nuclei [21]. However, the average size was 78.7 μm at 250 rpm, 82.7 μm at 300 rpm, 82.8 μm at 350 rpm and 79.6 μm at 400 rpm in the ultrasonic field. It was illustrated that the stirring rate had minor effect on the average size in the ultrasonic field, but the average size was smaller in the ultrasonic environment than that in silent environment. Prasad and Dalvi [27] believed that cavitation generated by ultrasound in the solution enhanced the micro-mixing, resulting in the increase of mass transfer rate and uniform supersaturation. Therefore, the nucleation rate was increased and the particle size was reduced.

The effect of stirring rate on the nucleation and growth rates was shown in Fig. 9. It can be seen that Fig. 9a and b showed the nucleation

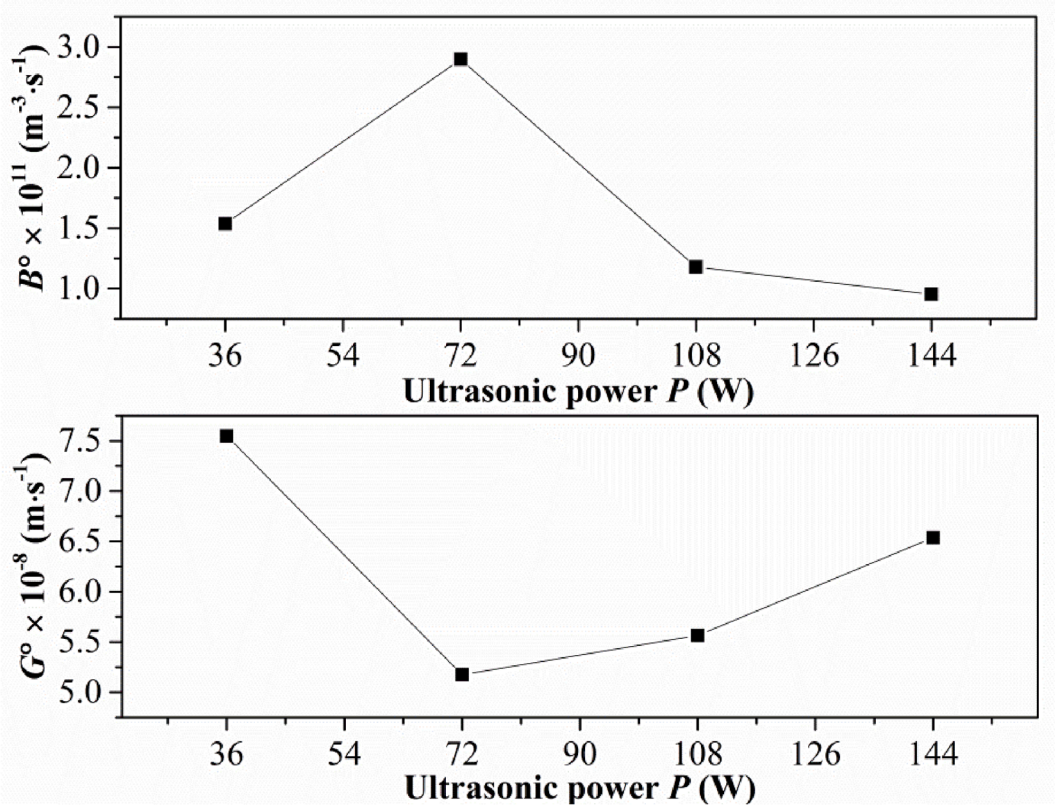

Fig. 12. Effect of ultrasonic power on the nucleation and growth rates (T = 306.15 K, N_p = 300 rpm, S = 1.3, ΔS= 0.816, t_0 = 16 min).

Table 3
Experimental data of anti-solvent crystallization of sucrose.

	T (K)	ΔS	M_T (kg·m^{-3})	N_p (rpm)	$B° \times 10^9$ (m^{-3}·s^{-1})
	306.15	0.649	215.88	300	0.97
	306.15	0.749	309.34	300	2.42
	306.15	0.908	355	300	2.29
	306.15	1.035	402.8	300	8.20
Without	306.15	1.204	421.4	300	13.4
ultrasound	306.15	0.816	339.66	250	3.72
	306.15	0.816	329.42	300	4.87
	306.15	0.816	287.24	350	5.19
	306.15	0.816	307.1	400	8.44
	298.15	0.816	323.16	300	3.87
	302.15	0.816	300.14	300	3.34
	306.15	0.816	329.42	300	4.87
	310.15	0.816	290.5	300	5.79
	306.15	0.649	308.38	300	14.0
	306.15	0.809	326.56	300	35.7
	306.15	0.935	395.82	300	118.4
	306.15	1.083	422.32	300	272.2
	306.15	1.225	455.78	300	965.6
With ultrasound	306.15	0.816	353.34	250	121.6
	306.15	0.816	333.48	300	117.9
	306.15	0.816	330.58	350	106.3
	306.15	0.816	362.98	400	161.1
	298.15	0.816	326.22	300	112.6
	302.15	0.816	338.2	300	113.9
	306.15	0.816	333.48	300	117.9
	310.15	0.816	354.86	300	183.0

Notes: P = 108 W, t_0 = 16 min.

Table 4
Kinetic parameters of anti-solvent crystallization of sucrose.

	ln k_B	E_a (J·mol^{-1})	i	j	l	Prob > F
Without ultrasound	6.9	20442.5	1.84	1.68	2.44	3.13 × 10^{-14}
With ultrasound	20.5	790.5	5.41	0.120	0.95	1.16 × 10^{-13}

Notes: P = 108 W, t_0 = 16 min.

and growth rates in silent environment. The mass transfer efficiency and nucleation rate were increased with the increase of stirring rate. The number of crystals generated per unit time was increased, and the growth rate was decreased. The nucleation and growth rates in the ultrasonic field were shown in Fig. 9c and d. The nucleation rate was decreased and the growth rate was increased at 250–350 rpm. The reason may be that when the stirring rate was low, the anti-solvent and sucrose solution were not completely mixed in a short time, resulting in an increase probability of local supersaturation [19]. In the ultrasonic field, the crystal nucleus was rapidly generated, resulting in the increase of nucleation rate and the decrease of growth rate. When the stirring rate reached 400 rpm, the influence on mass transfer was increased, and the nucleation rate was accelerated. During the experiment, increasing the stirring rate beyond 400 rpm was not feasible in the present setup as it may lead to splashing of the liquid onto the reactor walls giving problems in the overall crystallization operation and possibly errors in the measurements.

4.4. Effect of supersaturation of solution

The effect of supersaturation on the crystallization time was shown in Fig. 10. It was observed that Fig. 10a and b represented crystallization time in silent and ultrasonic environments. The crystallization time was reduced with the increase of supersaturation. Sheikh et al. [7] found that reduction in crystallization time was due to the increase in the

supersaturation level at constant temperature and stirring rate. Fig. 11 showed the effect of supersaturation on nucleation and growth rates. It can be seen that Fig. 11a and b showed the nucleation and growth rates in silent environment, while those in the ultrasonic environment were shown in Fig. 11c and d. The experimental results showed that the nucleation rate increased and the growth rate firstly increased and then decreased due to the increase of supersaturation. Higher concentrations of solution should produce a higher supersaturation level upon the mixing with the anti-solvent, and as a result, rate of nucleation increased [21]. Meanwhile, a large number of sucrose crystals were formed per unit time due to the increase of nucleation rate, which caused difficulty in the growth of the crystals and decrease in the growth rate of the crystals.

4.5. Effect of ultrasonic power

The effect of ultrasonic power on the nucleation and growth rates was shown in Fig. 12. When the ultrasonic power reached 72 W, the nucleation rate reached a maximum, which was 2.897×10^{11} $m^{-3}{\cdot}s^{-1}$, while the growth rate reached a minimum, which was 5.175×10^{-8} $m{\cdot}s^{-1}$. The observed increase of nucleation rate can be attributed to the cavitation effects including turbulence, higher heat and good mass transfer, leading to an increase in nucleation rate [16]. It was found that when the ultrasonic power exceeded 72 W, the nucleation rate was reduced and the growth rate was increased. The reason may be that high viscosity of sucrose solution weakened the cavitation effects.

4.6. Kinetics of anti-solvent crystallization of sucrose

The experimental data were shown in Table 3. According to the analysis, the nucleation rate was increased more than 14 times in the ultrasonic field. In order to simplify the calculations, the Eq. (1) was changed to:

$$lnB^{\circ} = lnk_B + (-\frac{E_a}{RT}) + ilnS + jlnM_T + llnN_P \quad (12)$$

After fitting the Eq. (12) to data in Table 3, the kinetic parameters k_B, E_a, i, j and l were obtained. The fitting results were shown in Table 4.

As it can be clearly seen from Table 4, the kinetic constant (k_B) was larger in the ultrasonic field than that in silent environment. The k_B value reflected the collision frequency of sucrose molecules. The larger k_B value, the higher the collision frequency of sucrose molecules. A lot of bubbles were produced when ultrasound was applied to a liquid. When the bubble collapsed, the internal environment of the crystallization reaction system may change, which may cause the change of k_B. Ultrasound can promote crystallization by increasing the collision frequency [28]. The calculation results showed that the activation energy of anti-solvent crystallization of sucrose was low in the ultrasonic field. Singh et al. [23] found that the activation energy of sucrose crystallization was estimated to be 21.0 $kJ{\cdot}mol^{-1}$ in the ultrasonic field. Ouiazzane et al. [5] found that the activation energy of sucrose crystallization was estimated to be 46.5 $kJ{\cdot}mol^{-1}$ in silent environment. Therefore, combined with the experimental results, ultrasound can reduce the activation energy. Compared with the silent environment, the larger i value in the ultrasonic field showed that ultrasound can effectively promote nucleation and shorten the crystallization time in a lower supersaturated environment [29]. In the ultrasonic field, the suspension density had a minor effect on nucleation rate, and the j value was smaller. The smaller l value indicated that ultrasound can effectively enhance the mass transfer capacity and weaken the influence of stirring rate on the mass transfer.

5. Conclusion

In the present work, the effects of temperature, stirring rate, supersaturation and ultrasonic power on the anti-solvent crystallization of sucrose were investigated, and the kinetics of anti-solvent crystallization of sucrose was further studied. It should be emphasized that the shape of sucrose crystals was irrelevant with the ultrasonic field. Under different typical conditions, the distributions of population density of sucrose crystals were similar. Based on the experimental data, the ASL model was used to calculate the values of n°, γ, b, G° and B°. All the b values were minus, indicating that the growth rates of sucrose crystals were related to their sizes. In the ultrasonic field, the nucleation rate of anti-solvent crystallization of sucrose was increased. At 298.15–306.15 K, the ultrasonic field had a minor effect on the nucleation rate. The effect was provoked at above 310.15 K. In silent environment, the nucleation rate was increased with the increase of stirring rate. In the ultrasonic field, the stirring rate of 400 rpm had a significant impact on the nucleation rate. The nucleation rate increased with the increase of supersaturation, while the growth rate firstly increased and then decreased. When the ultrasonic power reached 72 W, the nucleation rate reached a maximum while growth rate reached a minimum. The results of kinetics of anti-solvent crystallization of sucrose showed that the kinetic constant (k_B) was increased and activation energy (E_a) was reduced due to the introduction of ultrasound.

CRediT authorship contribution statement

Xuwei Zhong: Methodology, Validation, Formal analysis, Investigation, Writing – original draft, Writing – review & editing. **Chengdu Huang:** Resources, Writing – review & editing. **Lishan Chen:** Investigation. **Qinghong Yang:** Investigation. **Yongchun Huang:** Conceptualization, Methodology, Writing – review & editing, Project administration.

Declaration of Competing Interest

The authors declare that they have no known competing financial interests or personal relationships that could have appeared to influence the work reported in this paper.

Acknowledgements

This work was supported by the National Natural Science Foundation of China (No. 31660472). The authors thank Doctor Shuo Ai for his advice to the work presented here.

References

[1] T. Li, P. Zhou, T.P. Labuza, Effects of sucrose crystallization and moisture migration on the structural changes of a coated intermediate moisture food, Front. Chem. Sci. Eng. 3 (4) (2009) 346–350, https://doi.org/10.1007/s11705-009-0256-8.
[2] A. Borji, F.-E. Borji, A. Jourani, Sugar industry: effect of dextran concentrations on the sucrose crystallization in aqueous solutions, J. Eng. 2019 (2019) 1–6, https://doi.org/10.1155/2019/7987369.
[3] V.I. Tuzhilkin, M.G. Balykhin, S.M. Petrov, N.M. Podgornova, N.D. Lukin, V. A. Kovalyonok, Mathematical description of the isobaric vaporizing crystallization of sucrose, J. Food Eng. 306 (2021) 110614, https://doi.org/10.1016/j.jfoodeng.2021.110614.
[4] K. Huang, P.-J. Zhang, B. Hu, S.-J. Yu, Monitoring the effect of the dextran molecular weight on sucrose crystallization by focused beam reflectance measurement (FBRM), Sugar Technol. 18 (3) (2016) 325–332, https://doi.org/10.1007/s12355-015-0423-9.
[5] S. Ouiazzane, B. Messnaoui, S. Abderafi, J. Wouters, T. Bounahmidi, Modeling of sucrose crystallization kinetics: the influence of glucose and fructose, J. Cryst. Growth. 310 (15) (2008) 3498–3503, https://doi.org/10.1016/j.jcrysgro.2008.04.042.
[6] W. Tang, Y. Quan, J. Gong, J. Wang, Q. Yin, T. Li, Form selection of concomitant polymorphs: a case study informed by crystallization kinetics modeling, AIChE J. 67 (4) (2021), https://doi.org/10.1002/aic.v67.410.1002/aic.17129.
[7] A.R. Sheikh, S.R. Patel, Ultrasound assisted reactive crystallization of strontium sulfate, J. Cryst. Growth. 390 (2014) 114–119, https://doi.org/10.1016/j.jcrysgro.2013.11.029.
[8] C.-P. Ye, X.-X. Ding, W.-Y. Li, H. Mu, W. Wang, J. Feng, Determination of crystalline thermodynamics and behavior of anthracene in different solvents, AIChE J. 64 (6) (2018) 2160–2167, https://doi.org/10.1002/aic.16069.

[9] A. Markande, A. Nezzal, J. Fitzpatrick, L. Aerts, A. Redl, Influence of impurities on the crystallization of dextrose monohydrate, J. Cryst. Growth. 353 (1) (2012) 145–151, https://doi.org/10.1016/j.jcrysgro.2012.04.021.
[10] R.M. Wagterveld, L. Boels, M.J. Mayer, G.J. Witkamp, Visualization of acoustic cavitation effects on suspended calcite crystals, Ultrason. Sonochem. 18 (1) (2011) 216–225, https://doi.org/10.1016/j.ultsonch.2010.05.006.
[11] Z. Zhang, D.-W. Sun, Z. Zhu, L. Cheng, Enhancement of crystallization processes by power ultrasound: current state-of-the-art and research advances, Compr. Rev. Food Sci. Food Saf. 14 (4) (2015) 303–316, https://doi.org/10.1111/1541-4337.12132.
[12] N. Amara, B. Ratsimba, A. Wilhelm, H. Delmas, Growth rate of potash alum crystals: comparison of silent and ultrasonic conditions, Ultrason. Sonochem. 11 (1) (2004) 17–21, https://doi.org/10.1016/S1350-4177(03)00131-7.
[13] H.U. Rodríguez Vera, F. Baillon, F. Espitalier, P. Accart, O. Louisnard, Crystallization of α-glycine by anti-solvent assisted by ultrasound, Ultrason. Sonochem. 58 (2019) 104671, https://doi.org/10.1016/j.ultsonch.2019.104671.
[14] R.A. Khaire, P.R. Gogate, Understanding the role of different operating modes and ultrasonic reactor configurations for improved sonocrystallization of lactose, Chem. Eng. Process. 159 (2021) 108212, https://doi.org/10.1016/j.cep.2020.108212.
[15] R.A. Khaire, P.R. Gogate, Intensified recovery of lactose from whey using thermal, ultrasonic and thermosonication pretreatments, J. Food Eng. 237 (2018) 240–248, https://doi.org/10.1016/j.jfoodeng.2018.04.027.
[16] C.N. Gajendragadkar, P.R. Gogate, Ultrasound assisted intensified recovery of lactose from whey based on antisolvent crystallization, Ultrason. Sonochem. 38 (2017) 754–765, https://doi.org/10.1016/j.ultsonch.2016.08.011.
[17] V.S. Nalajala, V.S. Moholkar, Investigations in the physical mechanism of sonocrystallization, Ultrason. Sonochem. 18 (1) (2011) 345–355, https://doi.org/10.1016/j.ultsonch.2010.06.016.
[18] C. Devos, T. Van Gerven, S. Kuhn, Nucleation kinetics for primary, secondary and ultrasound-induced paracetamol crystallization, Cryst. Eng. Comm. 23 (30) (2021) 5164–5175.
[19] K.A. Ramisetty, A.B. Pandit, P.R. Gogate, Ultrasound-assisted antisolvent crystallization of benzoic acid: effect of process variables supported by theoretical simulations, Ind. Eng. Chem. Res. 52 (49) (2013) 17573–17582, https://doi.org/10.1021/ie402203k.
[20] P. Sayan, S.T. Sargut, B. Kiran, Effect of ultrasonic irradiation on crystallization kinetics of potassium dihydrogen phosphate, Ultrason. Sonochem. 18 (3) (2011) 795–800, https://doi.org/10.1016/j.ultsonch.2010.11.003.
[21] U.N. Hatkar, P.R. Gogate, Process intensification of anti-solvent crystallization of salicylic acid using ultrasonic irradiations, Chem. Eng. Process. 57–58 (2012) 16–24, https://doi.org/10.1016/j.cep.2012.04.005.
[22] S.Ü. Tanrıkulu, İ. Eroğlu, A.N. Bulutcu, S. Özkar, Crystallization kinetics of ammonium perchlorate in MSMPR crystallizer, J. Cryst. Growth. 208 (1-4) (2000) 533–540, https://doi.org/10.1016/S0022-0248(99)00434-0.
[23] K. Singh, S.P. Gupta, A. Kumar, A. Kumar, The effect of high intensity ultrasound (HIU) on the kinetics of crystallization of sucrose: elimination of latent period, Ultrason. Sonochem. 52 (2019) 19–24, https://doi.org/10.1016/j.ultsonch.2018.05.030.
[24] H.N. Kim, K.S. Suslick, The effects of ultrasound on crystals: sonocrystallization and sonofragmentation, Crystals 8 (2018) 280, https://doi.org/10.3390/cryst8070280.
[25] A.E. DeJong, R.W. Hartel, Impact of shear on crystallization behavior of sorbitol, J. Food Eng. 263 (2019) 30–37, https://doi.org/10.1016/j.jfoodeng.2019.05.021.
[26] J. Xue, C. Liu, M. Luo, M. Lin, Y. Jiang, P. Li, J. Yu, S. Rohani, Secondary nucleation and growth kinetics of aluminum hydroxide crystallization from potassium aluminate solution, J. Cryst. Growth. 507 (2019) 232–240, https://doi.org/10.1016/j.jcrysgro.2018.11.027.
[27] R. Prasad, S.V. Dalvi, Sonocrystallization: monitoring and controlling crystallization using ultrasound, Chem. Eng. Sci. 226 (2020) 115911, https://doi.org/10.1016/j.ces.2020.115911.
[28] Y. Hu, P. Guo, S. Wang, L. Zhang, Leaching kinetics of antimony from refractory gold ore in alkaline sodium sulfide under ultrasound, Chem. Eng. Res. Des. 164 (2020) 219–229, https://doi.org/10.1016/j.cherd.2020.09.029.
[29] C. Fang, W. Tang, S. Wu, J. Wang, Z. Gao, J. Gong, Ultrasound-assisted intensified crystallization of L-glutamic acid: crystal nucleation and polymorph transformation, Ultrason. Sonochem. 68 (2020) 105227, https://doi.org/10.1016/j.ultsonch.2020.105227.